Vol 16 No 2, February 2007
1009-1963/2007/16(02)/0456-07

Chinese Physics

© 2007 Chin. Phys. Soc.
and IOP Publishing Ltd

Intense laser beam guiding in self-induced electron cavitation channel in underdense plasmas*

Cang Yu(苍 宇)[a], Yu Wei(余 玮)[a],
Wu Hui-Chun(武慧春)[b], Xu Han(徐 涵)[a], and Tian You-Wei(田友伟)[a]

[a] *State Key Laboratory of High Field Laser Physics, Shanghai Institute of Optics and Fine Mechanics, Chinese Academy of Sciences, Shanghai* 201800, *China*

[b] *Laboratory of Optical Physics, Institute of Physics, Chinese Academy of Sciences, Beijing* 100080, *China*

(Received 9 June 2006; revised manuscript received 28 August 2006)

In underdense plasmas, the transverse ponderomotive force of an intense laser beam with Gaussian transverse profile expels electrons radially, and it can lead to an electron cavitation. An improved cavitation model with charge conservation constraint is applied to the determination of the width of the electron cavity. The envelope equation for laser spot size derived by using source-dependent expansion method is extended to including the electron cavity. The condition for self-guiding is given and illuminated by an effective potential for the laser spot size. The effects of the laser power, plasma density and energy dissipation on the self-guiding condition are discussed.

Keywords: relativistic self-focusing, ponderomotive self-channelling, self-induced electron cavitation, self-guiding

PACC: 4265, 5240D, 5240F

1. Introduction

Due to light diffraction, the penetration distance of less intense laser beams into substances is limited to the Rayleigh length. In many applications, such as laser accelerator,[1] x-ray laser,[2] and fast ignitor,[3,4] powerful lasers are required to propagate over distances considerably beyond the diffraction limit without significant energy losses. In underdense plasmas, stable self-guiding of laser due to relativistic self-focusing can occur when the laser power exceeds a critical power P_c.[5−7] Relativistic mass increase as well as the transverse ponderomotive expulsion of electrons results in an increase in the refractive index, of which the process is called relativistic self-focusing and ponderomotive self-channelling. For a sufficiently intense laser, the ponderomotive force can be strong enough to expel all the electrons within the core region of the beam, forming an electron cavity (EC).[8] Ions do not move in a short pulse duration because of their large mass, so the charge-separation field is brought into being. The width of EC is determined by the balance between the electrostatic force and the laser ponderomotive force. The laser pulse can be guided in the self-induced EC a long distance as it propagates in a waveguide with little energy attenuation. Such a plasma waveguide and the self-guided laser pulse have been observed in experiment.[9]

The propagation of relativistic laser pulse in plasmas is of a nonlinear process. The general method of solving the paraxial wave equation with nonlinear source terms is the source-dependent expansion (SDE) method,[10] which is used to derive an envelope equation for the laser spot size to describe the laser diffraction, self-focusing and guiding. By solving the envelope equation, the optical guiding by relativistic effects, ponderomotive effects, and preformed density channels can be studied.[11] The significant enhancement in the focusing effect by ponderomotive channelling, and the possible stable guiding of a powerful laser beam by a combination of relativistic focusing and ponderomotive channelling over extended distances have been given by Hafizi *et al.*[12] In their case, the laser power is not high enough to generate EC.

The decrease in the electron density within the core region due to the ponderomotive force will lead to a nonphysical negative density value as the force increases. It is regarded as the appearance of the EC. A simplified cavitation model is given by defining the

*Project supported by the National High Technology Inertial Confinement Fusion Foundation (Grant No 10335020/A0506), the National Natural Science Foundation of China (Grant Nos 10474081 and 10576035), and Natural Science Foundation of Shanghai (Grant No 05ZR14159).

'negative density' region as a cavity and replacing all negative values with zero. However, in this cavitation model, the charge conservation is broken in radial direction in which the net charge turns negative.[13] An improved cavitation model has been proposed to determine the actual width of the electron cavity with the constraint of charge conservation.[14] By using this modified EC model, the actual width of the cavity and the exact Bessel solution of the self-guided laser beam are obtained in uniform underdense and overdense plasmas.[14,15] The analysis shows that the stable self-guiding can take place.

In this paper, we apply the modified cavitation model[14] to determining the width of the self-induced EC, and use the SDE method to study analytically the propagation of the intense circularly polarized laser pulse with Gaussian transverse profile in a self-induced EC. The envelope equation for laser spot size in the presence of EC is derived, and the condition for the self-guiding is given. The effects of the laser power, plasma density and energy dissipation on the self-guiding condition are discussed.

2. Electron cavitation

For an intense circularly polarized laser pulse with Gaussian transverse profile propagating in an initially uniform underdense plasma, the transverse profile is $a(\rho) = (a_0 b_0/b)\exp(-\rho^2/2b^2)$, where $a = eA/mc^2$ is the normalized vector potential, ρ the radial coordinate, b the spot size, a_0 and b_0 are the vacuum amplitude and minimum spot size at focus, respectively. The space coordinates are normalized by c/ω_0, where ω_0 is the laser frequency and c is the speed of the light in vacuum. The transverse ponderomotive force expels electrons from the axis, while ions do not move in the short pulse duration, so that the electrostatic field arises from the charge separation. The electron density at the boundary of the channel is determined by the balance between the radial electrostatic and ponderomotive forces. For electrons with relativistic velocities, all thermal and collisional effects can be neglected, and the electron thermal pressure becomes negligible compared with the ponderomotive pressure. Furthermore, in our case, the laser pulse duration is long enough to disregard the phenomena caused by the longitudinal charge separation, such as wake field generation, but short enough to regard ion as motionless. In the stationary state, the ponderomotive force is balanced by the electrostatic force, and the state of the plasma can be described as

$$\partial_t n = -\nabla(nv) = 0, \tag{1}$$

$$\partial_t p = \nabla(\phi - \gamma) = 0, \tag{2}$$

$$\nabla^2\phi = n - Zn_\mathrm{i}, \tag{3}$$

where n is the electron density normalized by the critical density n_c, and v the electron fluid velocity normalized by c. p is the electron momentum normalized by mc, ϕ the electrostatic scalar potential normalized by mc^2/e, γ the relativistic factor, which is related to the normalized vector potential a by $\gamma = \sqrt{1+a^2}$ for a circularly polarized laser. n_i is the initial ion density, Z the charge state of ions, and the initial electron density $n_0 = Zn_\mathrm{i}$. The spacial derivative of γ equals the ponderomotive force. Equation (1) shows the charge conservation. Combining Eq.(2) and Eq.(3), the electron density can be written as

$$n = n_0 + \nabla_\perp^2\gamma, \tag{4}$$

where $\nabla = \nabla_\perp + \hat{\boldsymbol{z}}\partial_z \approx \nabla_\perp$ because in the paraxial approximation, the longitudinal component of the vector potential can be neglected. Here $\nabla_\perp^2 = \rho^{-1}\partial_\rho(\rho\partial_\rho)$ is in polar coordinates and $\hat{\boldsymbol{z}}$ is the unit vector in the at z-direction. Substituting the expressions of γ and a into Eq.(4) leads to the radial distribution of the electron density after the perturbation

$$n = n_0 - (a^2 b^{-4}/\gamma)[2b^2 - \rho^2(1+\gamma^{-2})], \tag{5}$$

and the corresponding electrostatic field distribution $E = -\partial_\rho\phi = (\rho/b^2)(\gamma - \gamma^{-1})$.

Nonphysical negative density value starts to appear at the beam centre when the ponderomotive force exceeds a certain value. The EC is generated, and the density within the EC is set as zero. The calculation of the cavity radius d by using the improved cavitation model starts from the total charge conservation as follows:

$$\int_0^\infty (n - Zn_\mathrm{i})\rho\mathrm{d}\rho = \int_0^d (-Zn_\mathrm{i})\rho\mathrm{d}\rho + \int_d^\infty \partial_\rho(\rho\partial_\rho\gamma)\mathrm{d}\rho = 0, \tag{6}$$

which reduces to

$$\partial_\rho\gamma|_{\rho=d} = \frac{aa'}{\sqrt{1+a^2}}|_{\rho=d} = -Zn_\mathrm{i}d/2. \tag{7}$$

Substituting $a(\rho)$ into Eq.(7) and replacing $Zn_{\rm i}$ with n_0 yield

$$(\gamma - \gamma^{-1})|_{\rho=d} = n_0 b^2/2, \tag{8}$$

where the unique value of d exists for a given b under a fixed laser power $P = \pi I b^2 = 11 \times 10^4 (a_0 b_0)^2$ TW. The electrostatic field inside the cavity becomes $E = \rho n_0/2$, whose value is exactly the same as that from the Gaussian Law.

For $P = 5.4$ TW, $b = 18$ and $n_0 = 0.01$, Fig.1 shows the radial profiles of the laser amplitude a (dash–dot) and its modulated distribution of electron density n derived from the two models. In the modified model (solid), the EC boundary lies at $d = 22$. Total charge along radial profile keeps conserved. There is a large electron density gradient at the EC boundary where the ponderomotive force is balanced by the strong electrostatic field from the positive charge in the cavity.[16] In the simplified model (dash), the EC boundary is at $d' = 15$. The total charge is negative. For a fixed laser power, $d' < d$, so the power required to generate the EC with a certain size must be overestimated in the simplified model.

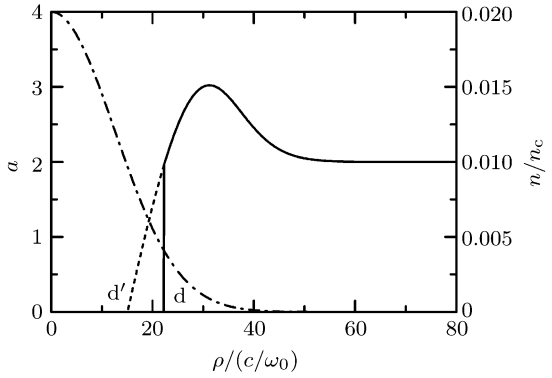


Fig.1. The radial profiles of the laser field a (dash–dot) and the corresponding electron density n distribution from the modified cavitation model (solid) and from the simplified cavitation model (dash) for $P = 5.4$ TW, $b = 18$, and $n_0 = 0.01$. d and d' are the boundaries of the EC in two different models.

Figure 2 shows the cavity radius as a function of laser spot size for different initial plasma densities and different laser powers. For a given laser power and plasma density, the EC appears when b is less than a critical spot size $b_{\rm c}$. It means that the threshold for the generation of EC is determined not only by the laser power, but also by the laser spot size. Taking $P = 5.4$ TW and $n_0 = 0.1$ (solid) for example, $b_{\rm c} = 11$. Increasing the laser power to $P = 21$ TW (dash) or decreasing the initial plasma density to $n_0 = 0.01$ (dash–dot) can lead to a higher $b_{\rm c}$. Because the higher laser power provides a stronger ponderomotive force, and the lower initial density is easier to empty. The EC is easier to generate as the high power laser propagates in low density plasmas. Figure 2 also shows that as the laser keeps focused, the radius of the cavity first increases due to the enhancement in the ponderomotive force. When most of the laser energy is confined within the cavity ($d > b$), the ponderomotive force at the cavity boundary becomes weaker than the electrostatic force, so that the radius of cavity decreases, with laser spot size sustaining the balance between two forces.

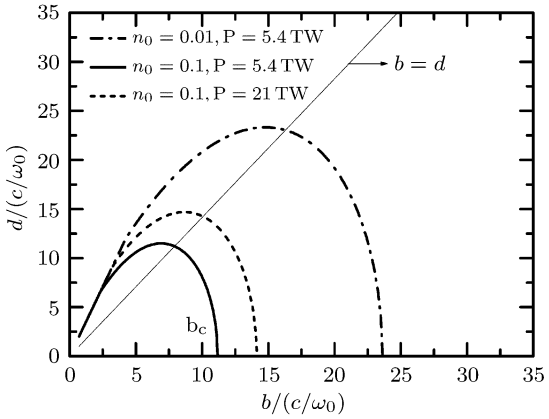


Fig.2. Dependences of radius of EC d on the laser spot size b for different plasma densities and different laser powers, with $b_{\rm c}$ being the critical laser spot size for the EC.

3. Envelope equation

In this section, we study the propagation of the laser pulse with Gaussian transverse profile in a self-induced EC. In an initially uniform plasma with refractive index η, by introducing $\xi = z - t$ and expressing the normalized vector potential as $a(\xi, z, \rho) = a(z, \rho)\exp(\mathrm{i}\xi)$, the paraxial wave equation of the vector potential can be written as [7]

$$(\nabla_\perp^2 + 2\mathrm{i}\partial_z)a = (1 - \eta^2)a. \tag{9}$$

The time coordinates are normalized by ω_0^{-1}. Substituting $\eta^2 = \epsilon_R + \mathrm{i}\epsilon_{\rm i}$ into Eq.(9) gives the energy conservation equation

$$\int_0^\infty (\partial_z |a|^2 + \epsilon_{\rm i}|a|^2)\rho \mathrm{d}\rho = 0, \tag{10}$$

where $\epsilon_{\rm i}$ is the imaginary part of the dielectric constant $\epsilon = \eta^2$, representing the coefficient of the energy consuming. Subject to the absence of energy dissipation, the refractive index is

$$\eta = \sqrt{\epsilon_{\rm R}} = \sqrt{1 - \frac{n}{\gamma}}, \tag{11}$$

where $\epsilon_{\rm R}$ is the real part of ϵ. Assuming that the transverse profile of the laser field remains approximately being of Gaussian form during propagation, and that a_0 and b_0 are independent of ρ and z, Eq.(9) can be solved by the SDE method.[10] It gives the envelope equation for laser spot size[12] as follows:

$$\partial_{zz} b = b^{-3} + 2b^{-1}G, \tag{12}$$

where the term of b^{-3} is responsible for natural diffraction and the term containing G, a function of η, is responsible for both relativistic and ponderomotive self-focusing. The solution of Eq.(12) describes the laser diffraction, self-focusing and guiding. In the absence of EC, the function G is given by[12]

$$\begin{aligned} G &= \frac{1}{2}\int_0^\infty {\rm d}\chi(1-\eta^2)(1-\chi)\exp(-\chi) \\ &= \frac{1}{2}\int_0^\infty {\rm d}\chi\frac{n}{\gamma}(1-\chi)\exp(-\chi), \end{aligned} \tag{13}$$

where $\chi = \rho^2/b^2$. In the presence of EC, the integration should start from the boundary of the cavity

$$\begin{aligned} G &= \frac{1}{2}\int_{\chi_d}^\infty {\rm d}\chi\frac{n}{\gamma}(1-\chi)\exp(-\chi) \\ &= \frac{{\rm e}^{-\chi_d}}{X^2-1}\left\{ n_0\left[(1+\chi_d)(1-X) + 2\ln\frac{1+X}{2}\right]\right. \\ &\quad \left. + \frac{1}{b^2}(2\ln X - X^2 + 1)\right\}, \end{aligned} \tag{14}$$

where $X = \sqrt{1+(a_0 b_0/b)^2\exp(-\chi_d)}$, $\chi_d = d^2/b^2$, and d is obtained from Eq.(8). As is known above, when $b > b_{\rm c}$ the cavity radius $d = 0$ and Eq.(14) reduces to Eq.(13). For a laser pulse propagating in the axial uniform plasmas without energy dissipation, G is only a function of b. Equation (12) can be rewritten as

$$\partial_{zz} b = -\partial_b U = b^{-3} + 2b^{-1}G, \tag{15}$$

where $U(b)$ is an effective potential for the laser spot size. By taking z as time, b as the displacement of the particle, and ${\rm d}b/{\rm d}z$ as the velocity, the evolution of spot size during laser propagation can be compared to a particle motion in an effective potential well.

Figure 3 shows the effective potential U as a function of spot size b. The laser power is $P = 5.4\,{\rm TW}$. For $n = 0.01$, the solid line is for G given by Eq.(14), and the dashed line is for G given by Eq.(13). Two lines separate at $b = b_{\rm c}$ as expected. For the $b < b_{\rm c}$ region, whether the EC is taken into consideration or not, the characteristic of the potential well can be directly affected. Ignoring the EC, Eq.(13) leads to the nonphysically continuous focusing of the laser spot as the potential keeps falling. No stationary state exists. Only when the EC is taken into account, will the whole system be energy conserved, that is, U has the bottom satisfying $\partial_b U|_{b=b_m} = 0$. A particle positioned at $b = b_m$ with zero initial velocity $\partial_z b|_{z=0} = 0$ will remain there. Correspondingly, a laser beam with an initial spot size $b_{\rm i} = b_0 = b_m$ will propagate, with $b = b_m$, a long distance without change. So, the laser self-guiding condition is $b_{\rm i} = b_0 = b_m$. For $n_0 = 0.01$, we have $b_m = 18$ and $d_m = 22$. In the following, we study only the case with $b_{\rm i} = b_0$, where the laser focal spot is right at the plasma boundary.

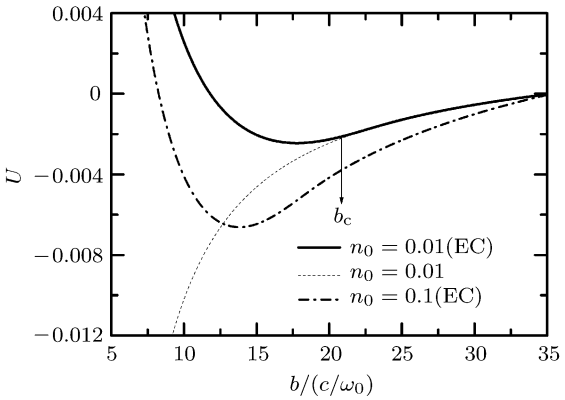


Fig.3. The effective potential $U(b)$ versus spot size b for $P = 5.4\,{\rm TW}$ in the two cases: in the presence of EC for $n_0 = 0.01$ (solid) and 0.1 (dash–dot) and in the absence of the EC for $n_0 = 0.01$ (dash).

Comparing to the case of $n = 0.1$ (dash–dot), the bottom of the potential well is found to always lie at $b < b_{\rm c}$, which means that the formation of the electron cavitation is the prerequisite for the self-guiding. The difference from the result in Ref.[12] is that the combination of the ponderomotive force with the relativistic focusing can realize the self-guiding in the absence of the EC. Because in Ref.[12], $\nabla_\perp^2 = \partial_\rho^2$ is not in the polar coordinates, which is unlike ours. Moreover, we note that d_m is always larger than b_m. The stable

self-guiding requires most of the laser energy to be confined within the self-induced cavity.

Figure 4 shows the dependences of b_m on n_0 for $P = 5.4\,\mathrm{TW}$ (solid) and 21 TW (dash). For the same laser power, b_m decreases as plasma density increases; for the same plasma density, b_m increases with laser intensity increasing. The dependences of b_m on n_0 and P are the same as the dependences of b_c on P and n_0.

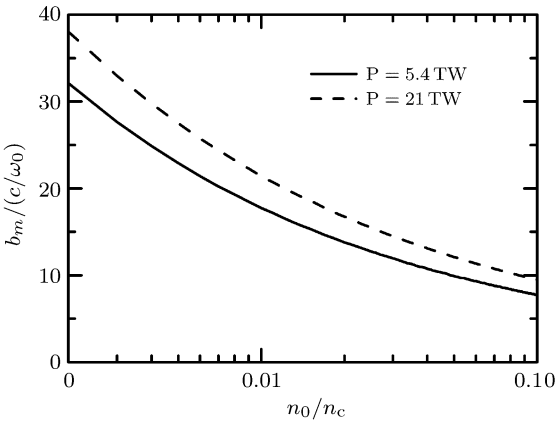


Fig.4. Dependences of self-guiding spot size b_m on plasma density n_0 for $P = 5.4$ (solid) and 21 TW (dash).

For $P = 5.4\,\mathrm{TW}$, $n_0 = 0.01$, when a laser pulse irradiates under $b_\mathrm{i} = 35$ that is not the self-guiding condition, the laser spot size (dashed curve) and cavity radius (solid curve) evolve with position z as shown in Fig.5.

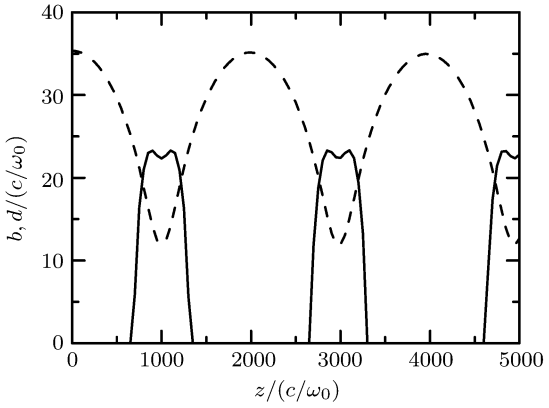


Fig.5. The spot size b (dash) and the corresponding radius of the EC d (solid) vs position z for $P = 5.4\,\mathrm{TW}$, $n_0 = 0.01$, and $b_0 = 35$.

The laser spot size oscillates between $b = 35$ and 12, around b_m. The radius of the EC varies with the laser spot size according to the relation shown in Fig.2. It can be illuminated by the effective potential shown in Fig.3. For a particle initially not staying at bottom, with an initial velocity $\mathrm{d}b/\mathrm{d}z|_{z=0}$ being not large enough to escape from the potential, it can oscillate around the potential bottom, subject to the energy conservation. Therefore, a laser beam not incident with self-guiding parameters will undergo an envelope oscillation around b_m.

4. Energy dissipation

During the propagation of an intense laser beam in an underdense plasma, there exist some energy dissipation processes, such as the laser energy transferring to electrons through the ponderomotive force. The length of the plasma channel will be limited by the energy dissipation. It can be easily understood that the laser beam will diffract quickly when P is less than P_c.

Equation (9) should be solved with Eq.(10) when the energy dissipation is taken into consideration. The basic assumption made in the SDE method is that a_0 and b_0 are independent of z, which means that P cannot change during propagation. Only when $\mathrm{d}P/\mathrm{d}z$ is small enough, can Eq.(12) be still valid. Substituting $P = \sigma(z)P_0$ into Eq.(12) yields the evolvement of spot size with energy dissipation. Here $P_0 = P(z=0) = 11 \times 10^{-4}(a_0 b_0)^2\,\mathrm{TW}$, and σ is found to obey $d_z\sigma = \epsilon_\mathrm{i}\sigma$. Taking $\epsilon_i = -10^{-3}$ for example, Fig.6(a) shows the power dissipation (dash–dot) and the laser spot size evolvement (solid) for $P_0 = 5.4\,\mathrm{TW}$, $n_0 = 0.01$. $b_i = b_m = 18$ is the self-guiding condition for P_0 and n_0. With energy dissipation, the laser power decreases as shown by the dash–dotted curve. The ponderomotive force becomes weaker and weaker, so that b_m decreases with P. Consequentially, conical shaped EC is generated. For other irradiation conditions, such as $b_\mathrm{i} = 16, 19$, and 20 around b_m, the laser spot size will oscillate around b_m for local P. The laser diffracts more quickly for $b_\mathrm{i} = 16$ and 20 since the derivation $\mathrm{d}b/\mathrm{d}z$ is very large. But for $b_\mathrm{i} = 18$ and 19, the diffraction is mainly due to the weak laser power. In Fig.6(a), $b_\mathrm{i} = 19$, which is quite close to b_m, is the optimal initial spot size for the longest laser channelling. The optimal b_0 changes with ϵ_i. For most values of ϵ_i, the optimal condition is $b_0 = b_m$ for P_0, and the propagation of the laser beam is most smooth for $b_0 = b_m$.

Figure 6(b) shows the laser spot size (solid) and

cavity radius (dash) for laser power $P_0 = 5.4$ and 8.4 TW under the self-guiding condition $b_\mathrm{i} = b_m$, i.e. $b_\mathrm{i} = 18$ for $P_0 = 5.4$ TW and $b_\mathrm{i} = 19$ for $P_0 = 8.4$ TW. As we expected, more powerful laser can be guided a longer distance in a plasma channel.

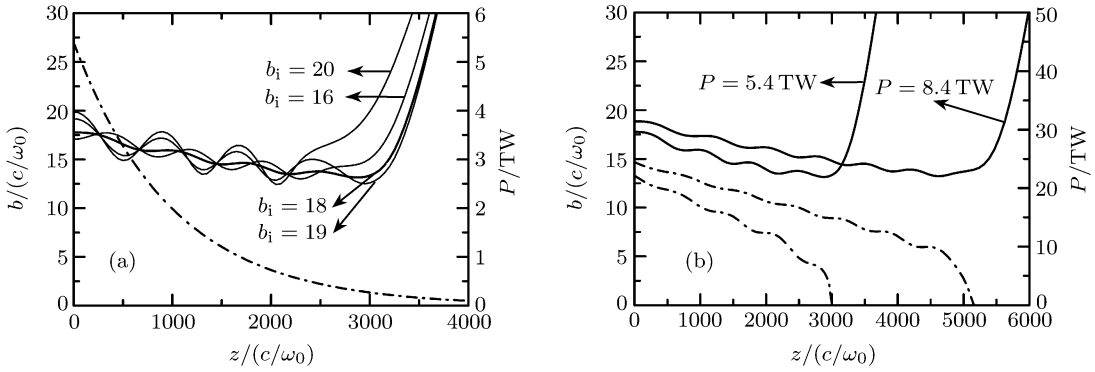


Fig.6. (a) In the presence of the energy dissipation of the laser power (dash–dot) with $P_0 = 5.4$ TW and $\epsilon_\mathrm{i} = -10^{-3}$ in a uniform plasma $n_0 = 0.01$, the evolution of the laser spot size b (solid) with position z under different incident parameters ($b_0 = 16, 18, 19, 20$) among which $b_0 = 18$ is the self-guiding condition for $P = 5.4$ TW and $n_0 = 0.01$; (b) The evolvement of the laser spot size b (solid) and the corresponding radius of the EC d (dash) of different laser powers with position z in a uniform plasma $n_0 = 0.01$ with $b_0 = b_m$. For $P_0 = 5.4$ TW, $b_0 = b_m = 18$, while for $P_0 = 8.4$ TW, $b_0 = b_m = 19$. $\epsilon_\mathrm{i} = -10^{-3}$ remains in two cases.

5. Conclusions

For an intense circularly polarized laser beam with Gaussian transverse profile propagating in an initially uniform underdense plasma, the ponderomotive force can be so strong that the EC can be generated near the axis. The appearance of the EC changes the properties of relativistic self-focusing and ponderomotive self-channelling dramatically. The intense laser beam can be self-guided in the EC.

The envelope equation in the presence of EC is solved to obtain the condition of self-guiding. The presence of EC is found to be a requirement for beam guiding, and the radius of the stable channel must be larger than the guided laser spot size.

With the energy dissipation taken into account, the conical shape channel is found and the boundary condition for the self-guiding still can be chosen to obtain the optimal channelling. The channel length increases with laser power increasing, and the diameter of the guided beam decreases as the plasma density increases. These results are in accordance with the experimental measurements.

References

[1] Esarey E, Sprangle P, Krall J and Ting A 1996 *IEEE Trans. Plasma Sci.* **24** 252
Umstadter D, Chen S Y, Maksimchuk A, Mourou G and Wagner R 1996 *Science* **273** 472
Chen M, Sheng Z M and Zhang J 2006 *Chin. Phys.* **15** 568
Chen M, Sheng Z M and Zhang J 2005 *Chin. Phys.* **14** 1407
Cang Y, Dong Q L, Wu H C, Sheng Z M, Yu W and Zhang J 2004 *Chin. Phys. Lett.* **21** 2414

[2] Burnett N H and Enright G D 1990 *IEEE J. Quant. Electron.* **26** 1797

[3] Tabak M, Hammer J, Glinsky M E, Kruer W L, Wilks S C, Woodworth J, Campbell E M, Perry M D and Mason R J 1994 *Phys. Plasmas* **1** 1626
Deutsch C, Furukawa H, Mima K, Murakami M and Nishihara K 1996 *Phys. Rev. Lett.* **77** 2483

[4] Pukhov A and Vehn J. M 1997 *Phys. Rev. Lett.* **79** 2686

[5] Borisov A B, Borovskiy A V, Korobkin V V, Prokhorov A M, Shiryaev O B, Shi X M, Luk T S, McPherson A, Solem J C, Boyer K and Rhodes C K 1992 *Phys. Rev. Lett.* **68** 2309
Sullivan A, Hamster H, Gordon S P and Falcone R W 1994 *Opt. Lett.* **19** 1544
Monot P, Auguste T, Gibbon P, Jakober F, Mainfray G, Dulieu A, Jacquet M Louis, Malka G and Miquel J L 1995 *Phys. Rev. Lett.* **74** 2953

[6] Sprangle P, Esarey E, Krall J and Joyce G 1992 *Phys. Rev. Lett.* **69** 2200
Vehn J Meyer-ter, Pukhov A and Sheng Z M 2001 *Atoms, Solids, and Plasmas in Super-Intense Laser Fields* (New York: Kluwer/Plenum) p167

[7] Esarey E, Sprangle P, Krall J and Ting A 1997 *IEEE J. Quant. Electron.* **33** 1879
[8] Sun G Z, Ott E, Lee Y C and Guzdar P 1987 *Phys. Fluids* **30** 526
[9] Chen S Y, Sarkisov G S, Maksimchuk A, Wagner R and Umstadter D 1998 *Phys. Rev. Lett.* **80** 2610
[10] Sprangle P, Ting A and Tang C M 1987 *Phys. Rev. Lett.* **59** 202
[11] Esarey E and Leemans W P 1999 *Phys. Rev.* E **59** 1082
Jha P, Wadhwani N, Upadhyaya A K and Raj G 2004 *Phys. Plasmas* **11** 3259
Hafizi B, Ting A, Hubbard R F, Sprangle P and Penano J R 2003 *Phys. Plasmas* **10** 1483
Sprangle P, Hafizi B, Penano J R, Hubbard R F, Ting A, Moore C I, Gordon D F, Zigler A, Kaganovich D and Antonsen T M Jr 2001 *Phys. Rev.* E **63** 056405
[12] Hafizi B, Ting A, Sprangle P and Hubbard R F 2000 *Phys. Rev.* E **62** 4120
[13] Feit M D, Komashko A M, Musher S L, Rubenchik A M and Turitsyn S K 1998 *Phys. Rev.* E **57** 7122
[14] Kim A, Tushentsov M, Cattani F, Anderson D and Lisak M 2002 *Phys. Rev.* E **65** 036416
[15] Shen B F and Yu M Y 2003 *Phys. Rev.* E **68** 026501
[16] Kim A, Tushentsov M, Anderson D and Lisak M 2002 *Phys. Rev. Lett.* **89** 095003